Chemistry and Physics of Lipids 231 (2020) 104937

Contents lists available at ScienceDirect

Chemistry and Physics of Lipids

journal homepage: www.elsevier.com/locate/chemphyslip

Synthesis and enantiospecific analysis of enantiostructured triacylglycerols containing n-3 polyunsaturated fatty acids

Marika Kalpio[a], Jóhann D. Magnússon[b], Haraldur G. Gudmundsson[a,b], Kaisa M. Linderborg[a], Heikki Kallio[a], Gudmundur G. Haraldsson[b], Baoru Yang[a,*]

[a] Food Chemistry and Food Development, Department of Biochemistry, University of Turku, FI-20014 Turku, Finland
[b] Science Institute, University of Iceland, Dunhaga 3, 107 Reykjavik, Iceland

ARTICLE INFO

Keywords:
Chemoenzymatic synthesis
Enantiostructured triacylglycerols
Enantiospecific separation
n-3 fatty acids
Recycling liquid chromatography

ABSTRACT

The stereospecific structure of triacylglycerols (TAGs) affects the bioavailability of fatty acids. Lack of enantiopure reference compounds and effective enantiospecific methods have hindered the stereospecific analysis of individual TAGs. Twelve novel enantiostructured AAB-type TAGs were synthesized containing one of the three n-3 polyunsaturated fatty acid: α-linolenic acid (ALA), eicosapentaenoic acid (EPA), or docosahexaenoic acid (DHA) in *sn*-1 or *sn*-3 position. These compounds formed six enantiomer pairs, which were separated with recycling high-performance liquid chromatography using chiral columns and UV detection. The chromatographic retention behavior of the enantiomers and the stereospecific elution order were studied. The enantiomer with an n-3 PUFA in the *sn*-1 position eluted faster than the enantiomer with the n-3 PUFA in the *sn*-3 position, regardless of the carbon chain length and number of double bonds of the PUFA. TAG enantiomers containing DHA exhibited highly different retention on the chiral column and were separated after the first column, whereas recycling was needed to separate the enantiomer pairs containing ALA or EPA. The system using two identical columns and one mobile phase, without sample derivatization, proved to be very effective also for peak purity assessment, confirming the enantiopurity of the synthesized structured TAGs being higher than 98 % (96 % ee).

1. Introduction

There is an increasing interest in the health effects of n-3 polyunsaturated fatty acids (PUFAs). α-Linolenic acid (18:3n-3, ALA) is an essential fatty acid and a precursor for synthesis of other long-chain n-3 PUFAs. Due to the low conversion of ALA to eicosapentaenoic acid (20:5n-3, EPA) and docosahexaenoic acid (22:6n-3, DHA), also EPA and DHA are often considered as essential components in the diet (Swanson et al., 2012). In addition to fatty acid composition, the positional distribution of the fatty acids in triacylglycerols (TAGs) is an important quality parameter as it affects the bioavailability of fatty acids.

In TAGs, the fatty acyl groups are covalently attached by ester bonds in the glycerol backbone in one of the three stereospecifically distinct locations termed *sn*-1, *sn*-2 and *sn*-3 (IUPAC-IUB Commission on Biochemical Nomenclature, 1977). When the two terminal primary hydroxyl groups of a glycerol are esterified with different fatty acids, the resulting TAG displays chiral asymmetry and thus, has two enantiomers. While enantiomers may differ only slightly in their chemical and physical properties, they are likely to have different biological activities in chiral environments like in the human body due to the three-dimensional structure-activity relationships (Smith, 2009). The stereospecific distribution of fatty acids in TAGs of natural fats and oils is under genetic control, making the positional distribution of fatty acids not random (Brockerhoff, 1971; Vichi et al., 2007).

Chirality of the other major food components like proteins and carbohydrates is well studied (Marchelli et al., 1996; Zawirska-Wojtasiak, 2006), whereas knowledge of the enantiomeric composition of lipids, TAGs in particular, is limited. To understand the health impact of nutritionally important fatty acids in natural TAG molecules in foods, reliable methods and tools are needed to study their enantiospecific location within the TAGs. Synthesis of novel enantiopure reference compounds is crucial for research on structure-activity relationship of TAGs and for development of analytical methods of TAG enantiomers (Kalpio et al., 2015; Kristinsson et al., 2014). Enantioselective HPLC is a promising technique with (Kalpio et al., 2015; Nagai et al., 2011) and without sample recycling systems (Lísa and Holčapek, 2013; Řezanka et al., 2018) to investigate the stereospecific distribution of fatty acids in TAGs of natural sources. Further research related to stereospecific

* Corresponding author at: Food Chemistry and Food Development Unit, Itäinen Pitkäkatu 4 A, 7th floor, Pharmacity, 20520 Turku, Finland.
E-mail address: baoru.yang@utu.fi (B. Yang).

https://doi.org/10.1016/j.chemphyslip.2020.104937
Received 17 May 2020; Received in revised form 10 June 2020; Accepted 20 June 2020
Available online 27 June 2020

separation of TAGs is still needed, to improve the separation of regioisomers and enantiomers in a single analysis.

In order to enable the bioavailability studies of n-3 PUFAs located in different *sn*-positions, various types of structured TAGs possessing EPA and DHA have been synthesized. These TAGs include normal-structured MLM (medium-long-medium) and similar ABA type TAGs possessing pure EPA or DHA located in the *sn*-2 position along with saturated even carbon number fatty acids ranging from C2 to C18 occupying the *sn*-1,3-terminal positions of the TAGs (Halldorsson et al., 2003; Haraldsson et al., 2000; Magnusson and Haraldsson, 2010). Furthermore, reversed-structured TAGs of the LML type have also been synthesized, possessing saturated fatty acids (SAFAs) in the *sn*-2 position and EPA or DHA located in the *sn*-1,3 positions (Gudmundsdottir et al., 2015; Magnusson and Haraldsson, 2012). These syntheses were all based on the use of a highly regioselective *Candida antarctica* lipase (CAL) immobilized as CAL-B, which played a key role in the syntheses by offering a full regiocontrol in terms of directing the SAFAs activated as vinyl esters exclusively into the less hindered terminal positions of glycerol. The same lipase offered similar regiocontrol in directing the n-3 PUFAs, activated as oxime esters, into the terminal positions of the glycerol backbone (Magnusson and Haraldsson, 2012). The use of activated fatty acids was essential for ensuring fast action of the lipase under mild temperature to avoid acyl migration side reaction (Compton et al., 2012; Laszlo et al., 2008), which is critical for the regiocontrol of the reactions. 1-(3-Dimethylaminopropyl)-3-ethylcarbodiimide hydrochloride (EDCI) was subsequently used as a coupling agent to chemically incorporate the n-3 PUFAs or SAFAs into the mid-position of the resulting 1,3-DAGs in highly efficient two-step chemoenzymatic processes.

In this study, our aim was to synthesize and chromatographically separate the enantiostructured AAB type TAGs containing one n-3 PUFA (ALA, EPA, or DHA) in *sn*-1 or *sn*-3 position. There are various reasons for the interest in enantiostructured TAGs possessing n-3 PUFA esterified to enantiospecific positions of the glycerol molecule. One was to design enantiostructured AAB type TAGs possessing pure ALA, EPA, or DHA in the *sn*-1, *sn*-2 or *sn*-3 position as unique TAG model molecules for investigating the impact of enantiospecific position of EPA and DHA on the bioavailability of these n-3 PUFAs in animals and humans (Linderborg et al., 2019). Symmetric TAGs constituting EPA and DHA in their *sn*-2 position are already available and fully characterized through the aforementioned synthesis, whereas the synthesis of the corresponding asymmetric TAGs has not been reported before. Secondly, we aim to extend our previous research on synthesis and enantiospecific separation of enantiostructured AAB type TAGs (Kalpio et al., 2015). In that study, the enantiomeric separation was performed on two AAB types of enantiostructured TAGs containing C12–C22 fatty acids with 0–2 double bonds (DBs), namely TAGs possessing two identical saturated fatty acids along with one unsaturated fatty acid, as well as TAGs possessing two identical unsaturated fatty acyl groups and one saturated one. In the current paper, we address a new challenge in the synthesis and analysis of enantiostructured AAB type TAGs possessing n-3 PUFAs with 3–6 DBs (ALA, EPA, or DHA) in one of the enantiomeric *sn*-1/*sn*-3 positions along with pure stearic (C18:0) or palmitic acids (C16:0) in the remaining positions. Separation of the resulting TAG enantiomers by the chiral-phase HPLC will produce novel information on elution order of TAG enantiomers containing n-3 PUFAs. Further, this will provide unique data for investigating the influence of carbon chain length and the number of DBs on the elution order of TAG enantiomers.

2. Materials and methods

2.1. Materials and methods of synthesis

2.1.1. General

^{1}H and ^{13}C nuclear magnetic resonance spectra were recorded on a Bruker Avance 400 spectrometer at 400 and 101 MHz, respectively, and referenced to the residual peak stated ($CDCl_3$, δ = 7.26/77.2). Chemical shifts (δ) are reported in parts per million (ppm) and the coupling constants (*J*) are reported to the nearest 0.5 Hz. The following abbreviations are used to describe the multiplicity: s, singlet; d, doublet; t, triplet; q, quartet; quin, quintet; dd, doublet of doublets; m, multiplet. Infrared spectra were conducted on a Thermo Nicolet FT-IR iS10 Spectrophotometer on a KBr pellet (crystalline material) or as a neat liquid (oils). Melting points were determined on a Büchi 520 melting point apparatus and are uncorrected. The high-resolution mass spectra (HRMS) were acquired on a Bruker micrOTOF-Q mass spectrometer. All data analysis was done on Bruker software. Optical activity measurements were performed on an Autopol^{R} V Automatic Polarimeter from Rudolph Research Analytical using a 40T-2.5-100-0.7 Temp Trol™ polarimetric cell with 2.5 mm inside diameter, 100 mm optical path length and 0.7 mL volume with c referring to g sample/100 mL.

The immobilised *Candida antarctica* lipase (Novozym 435; CAL-B) was supplied as a gift from Novozymes A/S (Bagsvaerd, Denmark). All chemicals and solvents were used without further purification unless otherwise stated. (*R*)-(-)-2,2-Dimethyl-1,3-dioxolane-4-methanol (*R*-solketal, 98 % purity and 99 % ee) and (*S*)-(+)-2,2-Dimethyl-1,3-dioxolane-4-methanol (*S*-solketal, 98 % purity and 99 % ee) were purchased from Sigma-Aldrich (Steinheim, Germany). EDCI (1-(3-dimethylaminopropyl)-3-ethylcarbodiimide hydrochloride, 98 %) was obtained commercial grade from Sigma-Aldrich (Steinheim, Germany) and 4-dimethylaminopyridine (DMAP, 99 %) from Acros Organics (Geel, Belgium). Benzyl bromide (98 %), sodium hydride (60 % dispersion in mineral oil) and 10 % palladium on carbon catalyst were from Sigma-Aldrich (Steinheim). ALA, EPA, DHA, palmitic acid and stearic acid were all obtained as free acids in high (>99 %) purity from Larodan Fine Chemicals (Malmö, Sweden). For the larger scale material intended for the animal studies, DHA (≥ 95 %) was obtained as ethyl ester from Pronova BioPharma (Sandefjord, Norway) and hydrolysed to the corresponding free acid (Haraldsson et al., 2000). Dichloromethane and ethyl acetate were obtained as HPLC grade from Sigma-Aldrich (Steinheim, Germany), *n*-hexane as p.a. from Merck (Darmstadt, Germany), petroleum ether, boiling range 40 − 60 °C, and ethanol (99.8 %) from Honeywell (Seelze, Germany). Dichloromethane was dried over CaH_2 under dry nitrogen atmosphere. Tetrahydrofuran for analysis was obtained from Acros Organics (Geel, Belgium) and dried over Na wire in presence of benzophenone under dry nitrogen atmosphere. Column chromatography was performed on Silica gel 60 (Silicycle, Ontario, Canada). Reactions were monitered by TLC on Silica gel 60 F254 (Silicycle, Ontario, Canada), with detection by quenching of fluorescence and/or with phosphomolybdic acid in ethanol.

2.1.2. Syntheses

2.1.2.1. 3-O-Benzyl-sn-glycerol, (R)-1. Sodium hydride (13.4 g, 60 wt % dispersion in mineral oil, 336 mmol, 3.0 equiv.) was treated several times with dry pet. ether using a syringe to remove the mineral oil. To the resulting suspension in THF (280 mL) at 0 °C was added (*S*)-solketal (14.0 mL, 112 mmol, 1.0 equiv.) dropwise *via* syringe. The cooling bath was removed, and the resulting suspension was stirred at room temperature for 1 h before being cooled back to 0 °C followed by dropwise addition of benzyl bromide (15.9 mL, 134 mmol, 1.2 equiv.). The resulting mixture was brought to reflux and stirred for 4 h after which it was cooled to 0 °C, diluted carefully with EtOH (172 mL), followed by addition of a 2.0 M aqueous solution of HCl (168 mL). After stirring at 80 °C for 1 h, the resulting mixture was cooled to room temperature and quenched by addition of a saturated aqueous solution of $NaHCO_3$ (300 mL). The organic layer was separated and the aqueous layer further extracted with EtOAc (3 × 200 mL), the combined organic layers were dried over anhydrous Na_2SO_4, filtered and concentrated *in vacuo* to give the crude product which was purified *via* column chromatography (petroleum ether / EtOAc (50 %) → petroleum ether / EtOAc (80 %)) to give (*R*)-**1** (19.8 g, 109 mmol, 97 %) as a yellow oil; $[\alpha]_D^{24}$ +5.10 (*c* 19.6, $CHCl_3$); $\mathbf{R_f}$ 0.20 (petroleum ether / EtOAc (70 %)); **^{1}H NMR** (400 MHz, $CDCl_3$) δ_H 7.40 − 7.27 (5H, m, Ar*H*), 4.56 (2H,

s, OCH_2Ar), 3.95 − 3.85 (1H, m, CHOH), 3.77 − 3.69 (1H, m, CH_2OH), 3.67 − 3.62 (1H, m, CH_2'OH), 3.59 (1H, dd, J = 9.5 and 4.0 Hz, CH_2OBn), 3.55 (1H, dd, J = 9.5 and 6.0 Hz, CH_2'OBn), 2.57 (1H, d, J = 4.5 Hz, OH), 2.06 (1H, app. t, J = 6.0 Hz, OH); **^{13}C NMR** (101 MHz, $CDCl_3$) δ_C 137.7, 128.5(2), 127.9, 127.8(2), 73.6, 71.8, 70.6, 64.1.

Spectroscopic data was in agreement with that obtained for (*S*)-**1** as previously reported (Kristinsson et al., 2014).

*2.1.2.2. 1-O-Benzyl-sn-glycerol, (S)-**1**.* (*S*)-**1** was prepared in accordance with (*R*)-**1**. Spectroscopic data was identical to (*R*)-**1** and in agreement with that as previously reported (Kristinsson et al., 2014). For more details, please see *Supplementary material*.

2.1.2.3. General procedure a: enzymatic di-acylation procedure. A mixture of benzyl-protected glycerol (1.0 equiv.) and saturated fatty acid (2.1 equiv.) were brought to a melt (80 °C) followed by addition of an immobilized *Candida antarctica* lipase B (CAL-B) (5.0–10.0 wt % of total mass). Next, vacuum was carefully applied and the resulting suspension stirred at 80 °C at a rate not damaging the lipase carrier material for 16 − 48 h before being cooled to room temperature. The resulting solid material was dissolved in CH_2Cl_2, the lipase separated by filtration and the filtrate concentrated *in vacuo* to give the crude product which was purified by recrystallization.

*2.1.2.4. 3-O-Benzyl-1,2-dihexadecanoyl-sn-glycerol, (S)-**2a**.* (*S*)-**2a** was prepared using General Procedure A, with (*R*)-**1** (3.15 g, 17.3 mmol), palmitic acid (9.1 g, 35.5 mmol) and CAL-B (1.20 g, 10.0 wt%) with a reaction time of 16 h. Purification by recrystallization from hot ethanol gave (*S*)-**2a** (9.87 g, 15.0 mmol, 87 %) as colourless crystals; **M.p.** 42.5–43.4 °C; $[\alpha]_D^{25}$ +6.52 (*c* 2.3, $CHCl_3$); $\mathbf{R}_f$ 0.30 (petroleum ether / EtOAc (10 %)); **IR** (thin film, ν_{max} / cm^{-1}) 2917, 2849, 1731; **^{1}H NMR** (400 MHz, $CDCl_3$) δ_H 7.38 − 7.27 (5H, m, PhH), 5.28 − 5.19 (1H, m, CHOCO), 4.52 (1H, d, J = 12.0 Hz, OCH_2Ph), 4.51 (1H, d, J = 12.0 Hz, OCH_2'Ph), 4.34 (1H, dd, J = 12.0 and 4.0 Hz, CH_2OCO), 4.19 (1H, dd, J = 12.0 and 6.5 Hz, CH_2'OCO), 3.60 (1H, dd, J = 11.5 and 5.0 Hz, CH_2OBn), 3.57 (1H, dd, J = 11.5 and 5.0 Hz, CH_2'OBn), 2.32 (2H, t, J = 7.5 Hz, CH_2COO), 2.27 (2H, t, J = 7.5 Hz, CH_2COO), 1.67 − 1.51 (4H, m, 2 × CH_2CH$_2$COO), 1.37 − 1.18 (48H, m, 24 × CH_2), 0.88 (6H, t, J = 6.5 Hz, 2 × CH_3); **^{13}C NMR** (101 MHz, $CDCl_3$) δ_C 173.4, 173.2, 137.7, 128.4(2), 127.8, 127.6(2), 73.3, 70.0, 68.3, 62.7, 34.3, 34.1, 31.9, 29.7, 29.6, 29.5, 29.4, 29.3, 29.2, 29.1, 29.0, 25.0, 24.9, 22.7, 14.1; **HRMS** (ESI+) calc. for $C_{42}H_{74}O_5Na$ [M + Na]$^+$ 681.5428, found 681.5410.

*2.1.2.5. 1-O-Benzyl-2,3-dihexadecanoyl-sn-glycerol, (R)-**2a**.* (*R*)-**2a** was prepared using General Procedure A, and the spectroscopic data was identical to that obtained for (*S*)-**2a**. For further details, please see *Supplementary material*.

2.1.2.6. 3-O-Benzyl-1,2-dioctadecanoyl-sn-glycerol, (S)-2b. (*S*)-**2b** was prepared using General Procedure A, with (*R*)-**1** (12.1 g, 66.6 mmol), stearic acid (40.0 g, 141 mmol) and CAL-B (2.60 g, 5.0 wt %) with a reaction time of 48 h. Purification by recrystallization from hot ethanol gave (*S*)-**2b** (46.0 g, 64.3 mmol, 97 %) as colourless crystals; **M.p.** 49.7–50.4 °C; $[\alpha]_D^{27}$ +6.08 (*c* 20.3, $CHCl_3$); $\mathbf{R}_f$ 0.87 (petroleum ether / EtOAc (40 %)); **IR** (thin film, ν_{max} / cm^{-1}) 2917, 2847, 1747, 1730; **^{1}H NMR** (400 MHz, $CDCl_3$) δ_H 7.38 − 7.26 (5H, m, PhH), 5.28 − 5.18 (1H, m, CHOCO), 4.52 (1H, d, J = 12.0 Hz, OCH_2Ph), 4.51 (1H, d, J = 12.0 Hz, OCH_2'Ph), 4.35 (1H, dd, J = 12.0 and 4.0 Hz, CH_2OCO), 4.19 (1H, dd, J = 12.0 and 6.5 Hz, CH_2'OCO), 3.60 (1H, dd, J = 11.5 and 5.0 Hz, CH_2OBn), 3.57 (1H, dd, J = 11.5 and 5.0 Hz, CH_2'OBn), 2.32 (2H, t, J = 7.5 Hz, CH_2COO), 2.28 (2H, t, J = 7.5 Hz, CH_2COO), 1.68 − 1.55 (4H, m, 2 × CH_2CH$_2$COO), 1.38 − 1.18 (56H, m, 28 × CH_2), 0.88 (6H, t, J = 6.5 Hz, 2 × CH_3); **^{13}C NMR** (101 MHz, $CDCl_3$) δ_C 173.6, 173.3, 137.9, 128.6(2), 127.9, 127.8(2), 73.5, 70.2, 68.4, 62.8, 34.5, 34.3, 32.1, 29.9, 29.8, 29.7, 29.6, 29.5, 29.4, 29.3, 29.2, 29.1, 25.1, 25.0, 22.9, 14.3; **HRMS** (ESI+) calc. for $C_{46}H_{82}O_5Na$ [M + Na]$^+$ 737.6054, found 737.6051.

Spectroscopic data was in agreement with that as previously reported (Kristinsson et al., 2014).

*2.1.2.7. 1-O-Benzyl-2,3-dioctadecanoyl-sn-glycerol, (R)-**2b**.* (*R*)-**2b** was prepared using General Procedure A, and spectroscopic data was identical to that obtained for (*S*)-**2b**. For more details, please see Supplementary material.

2.1.2.8. General procedure B: catalytic hydrogenolysis procedure. An oven-dried round-bottom flask, equipped with a stirrer bar, was charged with benzyl-protected glycerol (1.0 equiv.) and Pd/C (10 wt % Pd, 3 − 5 mol%). The flask was evacuated, filled with nitrogen, the appropriate volume of hexane (10.0 mL / mmol substrate) and THF (1.0 mL / mmol substrate) added, and the flask was purged with hydrogen before a single drop of $HClO_3$ (70 wt% in water) was added. Hydrogenation (H_2 balloon) was conducted at r.t. with vigorous stirring until completion (monitored by TLC). The reaction mixture was then diluted with THF, filtered through Celite and concentrated *in vacuo* to give the crude product which was purified by recrystallization.

*2.1.2.9. 1,2-Dihexadecanoyl-sn-glycerol, (S)-**3a**.* (*S*)-**3a** was prepared using General Procedure B, with (*S*)-**2a** (9.85 g, 14.9 mmol), Pd/C (792 mg, 10 wt% Pd, 0.75 mmol. 5.0 mol %) and $HClO_3$ (single drop, 70 wt % in water) in hexane (150 mL) and THF (15 mL), with a reaction time of 4 h. Purification by recrystallization from hot hexane gave (*S*)-**3a** (8.24 g, 14.5 mmol, 97 %) as colourless crystals;

^{1}H NMR (400 MHz, $CDCl_3$) δ_H 5.08 (1H, app. quin, J = 5.0 Hz, CHOCO), 4.32 (1H, dd, J = 12.0 and 4.5 Hz, CH_2OCO), 4.24 (1H, dd, J = 12.0 and 5.5 Hz, CH_2'OCO), 3.76 − 3.70 (2H, m, CH_2OH), 2.27 (4H, app. q, J = 7.5 Hz, 2 × CH_2COO), 2.01 (1H, t, J = 6.5 Hz, OH), 1.68 − 1.57 (4H, m, 2 × CH_2CH$_2$COO), 1.37 − 1.19 (48H, m, 24 × CH_2), 0.88 (6H, t, J = 6.5 Hz, 2 × CH_3); **^{13}C NMR** (101 MHz, $CDCl_3$) δ_C 173.8, 173.4, 72.1, 62.0, 61.6, 34.3, 34.1, 31.9, 29.8, 29.7, 29.6, 29.5, 29.4, 29.3, 29.2, 29.1, 29.0, 25.0, 24.9, 22.7, 14.1

Spectroscopic data was in agreement with that as previously reported (Kristinsson et al., 2014).

*2.1.2.10. 2,3-Dihexadecanoyl-sn-glycerol, (R)-**3a**.* (*R*)-**3a** was prepared using General Procedure B. Spectroscopic data was identical to (*S*)-**3b** and in agreement with that as previously reported (Kristinsson et al., 2014). For further details, please see Supplementary material.

*2.1.2.11. 1,2-Dioctadecanoyl-sn-glycerol, (S)-**3b**.* (*S*)-**3b** was prepared using General Procedure B, with (*S*)-**2b** (2.05 g, 2.80 mmol), Pd/C (100 mg, 10 wt % Pd, 94.0 µmol. 3.5 mol %) and $HClO_3$ (single drop, 70 wt % in water) in hexane (30 mL) and THF (3.0 mL), with a reaction time of 15 min. Purification by recrystallization from hot hexane gave (*S*)-**3b** (1.53 g, 2.45 mmol, 88 %) as colourless crystals;

^{1}H NMR (400 MHz, $CDCl_3$) δ_H 5.15 − 5.00 (1H, m, CHOCO), 4.32 (1H, dd, J = 12.0 and 4.5 Hz, CH_2OCO), 4.23 (1H, dd, J = 12.0 and 5.5 Hz, CH_2'OCO), 3.81 − 3.63 (2H, m, CH_2OH), 2.34 (2H, t, J = 7.5 Hz, CH_2COO), 2.32 (2H, t, J = 7.5 Hz, CH_2COO), 2.03 (1H, t, J = 6.5 Hz, OH), 1.68 − 1.58 (4H, m, 2 × CH_2CH$_2$COO), 1.38 − 1.18 (56H, m, 28 × CH_2), 0.88 (6H, t, J = 6.5 Hz, 2 × CH_3); **^{13}C NMR** (101 MHz, $CDCl_3$) δ_C 173.9, 173.6, 72.3, 62.2, 61.7, 34.5, 34.3, 32.1, 29.9, 29.8, 29.7, 29.6, 29.5, 29.4, 29.3, 29.2, 25.1, 25.0, 22.9, 14.3.

Spectroscopic data was in agreement with that as previously reported (Kristinsson et al., 2014).

*2.1.2.12. 2,3-Dioctadecanoyl-sn-glycerol, (R)-**3b**.* (*R*)-**3b** was prepared using General Procedure B, and the spectroscopic data was identical to (*S*)-**3b** and in agreement with that as previously reported (Kristinsson et al., 2014). For further details, please see *Supplementary material*.

2.1.2.13. General procedure C: Steglich esterification procedure. To a solution of diacylglycerol (1.0 equiv), *N*-(3-dimethylaminopropyl)-*N*'-ethylcarbodiimide hydrochloride (EDCI) (1.1–1.2 equiv.) and 4-(dimethylamino)pyridine (DMAP) (0.2 − 0.4 equiv.) in CH_2Cl_2 (2.5 mL / mmol substrate), was added the corresponding unsaturated fatty acid (1.05–1.2 equiv.). After stirring overnight at room temperature, the resulting crude mixture was directly purified *via* column chromatography.

*2.1.2.14. 1,2-Dihexadecanoyl-3-(9Z,12Z,15Z)-octadeca-9,12,15-trienoyl)-sn-glycerol, (R)-**4a**.* (*R*)-**4a** was prepared using General Procedure C, with (*S*)-**3a** (195 mg, 0.34 mmol), ALA (109 μL, 0.36 mmol, 1.05 equiv.), EDCI (80.0 mg, 0.42 mmol, 1.2 equiv.) and DMAP (9.0 mg, 0.07 mmol, 0.2 equiv.) in CH_2Cl_2 (0.85 mL). Purification *via* column chromatography (petroleum ether / EtOAc (5 %) gave (*R*)-**4a** (273 mg, 0.33 mmol, 97 %) as a white waxy solid (with a tint of yellow);

$[\alpha]_D^{25}$ + 0.02 (*c* 16.3, $CHCl_3$); $\mathbf{R}_f$ 0.74 (petroleum ether / EtOAc (10 %)); **IR** (thin film, ν_{max} / cm^{-1}) 3012, 2917, 2849, 1732; **^{1}H NMR** (400 MHz, $CDCl_3$) δ_H 5.50 − 5.25 (7H, m, 6 × =C*H* and C*H*OCO), 4.29 (2H, dd, *J* = 12.0 and 4.0 Hz, 2 × CH_2OCO), 4.14 (2H, dd, *J* = 12.0 and 6.0 Hz, 2 × CH_2'OCO), 2.81 (4H, app. t, *J* = 6.5 Hz, 2 × =CCH_2C=), 2.37 − 2.26 (6H, m, 3 × CH_2COO), 2.14 − 2.01 (4H, m, =CCH_2CH$_3$ and = CCH_2CH$_2$), 1.67 − 1.55 (6H, m, 3 × CH_2CH$_2$COO), 1.39 − 1.18 (56H, m, 28 × CH_2), 0.98 (3H, t, *J* = 7.5 Hz, =CCH$_2$CH_3), 0.88 (6H, t, *J* = 6.5 Hz, 2 × CH_3); **^{13}C NMR** (101 MHz, $CDCl_3$) δ_C 173.4, 173.3, 173.0, 132.1, 130.4, 128.4, 128.3, 127.9, 127.3, 69.0, 62.3 (2), 34.4, 34.3, 34.2, 32.1, 30.1, 30.0, 29.9, 29.8, 29.7, 29.6, 29.5, 29.4, 29.3, 29.2, 29.1, 29.0, 27.4, 25.8, 25.7, 25.1, 25.0, 24.9, 22.8, 20.7, 14.4, 14.3; **HRMS** (ESI+) calc. for $C_{53}H_{96}O_6Na$ [M + Na]$^+$ 851.7099, found 851.7094.

*2.1.2.15. 2,3-Dihexadecanoyl-1-(9Z,12Z,15Z)-octadeca-9,12,15-trienoyl)-sn-glycerol, (S)-**4a**.* (*S*)-**4a** was prepared using General Procedure C, and the spectroscopic data was identical to that obtained for (*R*)-**4a**. For further details, please see *Supplementary material*.

*2.1.2.16. 1,2-Dioctadecanoyl-3-(9Z,12Z,15Z)-octadeca-9,12,15-trienoyl)-sn-glycerol, (R)-**4b**.* (*R*)-**4b** was prepared using General Procedure C, with (*S*)-**3b** (302 mg, 0.48 mmol), ALA (168 μL, 0.56 mmol, 1.15 equiv.), EDCI (114 mg, 0.60 mmol, 1.2 equiv.) and DMAP (14.0 mg, 0.12 mmol, 0.2 equiv.) in CH_2Cl_2 (1.2 mL). Purification *via* column chromatography (petroleum ether / EtOAc (5 %) gave (*R*)-**4b** (411 mg, 0.46 mmol, 96 %) as a white waxy solid (with a tint of yellow);

$[\alpha]_D^{25}$ + 0.02 (*c* 21.7, $CHCl_3$); $\mathbf{R}_f$ 0.70 (petroleum ether / EtOAc (10 %)); **IR** (thin film, ν_{max} / cm^{-1}) 3012, 2917, 2849, 1733; **^{1}H NMR** (400 MHz, $CDCl_3$) δ_H 5.45 − 5.23 (7H, m, 6 × =C*H* and C*H*OCO), 4.29 (2H, dd, *J* = 12.0 and 4.0 Hz, 2 × CH_2OCO), 4.14 (2H, dd, *J* = 12.0 and 6.0 Hz, 2 × CH_2'OCO), 2.87 − 2.74 (4H, m, 2 × =CCH_2C=), 2.35 − 2.26 (6H, m, 3 × CH_2COO), 2.14 − 2.01 (4H, m, =CCH_2CH$_3$ and = CCH_2CH$_2$), 1.67 − 1.56 (6H, m, 3 × CH_2CH$_2$COO), 1.38 − 1.18 (64H, m, 32 × CH_2), 0.98 (3H, t, *J* = 7.5 Hz, =CCH$_2$CH_3), 0.88 (6H, t, *J* = 7.0 Hz, 2 × CH_3); **^{13}C NMR** (101 MHz, $CDCl_3$) δ_C 173.5, 173.4, 173.0, 132.1, 130.4, 128.5, 128.4, 127.9, 127.3, 69.0, 62.3 (2), 34.4, 34.3, 34.2, 32.1, 30.1(2), 30.0(2), 29.9, 29.8, 29.7, 29.6, 29.5, 29.4, 29.3, 29.2, 29.1, 29.0, 27.4, 25.8, 25.7, 25.1, 25.0, 24.9, 22.8, 20.7, 14.4, 14.3; **HRMS** (ESI+) calc. for $C_{57}H_{104}O_6Na$ [M + Na]$^+$ 907.7725, found 907.7717.

*2.1.2.17. 2,3-Dioctadecanoyl-1-(9Z,12Z,15Z)-octadeca-9,12,15-trienoyl)-sn-glycerol, (S)-**4b**.* (*S*)-**4b** was prepared using General Procedure C, and the spectroscopic data was identical to that obtained for (*R*)-**4b**. For further details, please see *Supplementary material*.

*2.1.2.18. 3-(5Z,8Z,11Z,14Z,17Z)-Eicosa-5,8,11,14,17-pentaenoyl)-1,2-dihexadecanoyl-sn-glycerol, (R)-**5a**.* (*R*)-**5a** was prepared using General Procedure C, with (*S*)-**3a** (100 mg, 0.17 mmol), EPA (64.0 μL, 0.19 mmol, 1.1 equiv.), EDCI (39.0 mg, 0.20 mmol, 1.2 equiv.) and DMAP (8.0 mg, 0.07 mmol, 0.4 equiv.) in CH_2Cl_2 (0.4 mL). Purification *via* column chromatography (petroleum ether / EtOAc (5 %) gave (*R*)-**4a** (145 mg, 0.17 mmol, 99 %) as a white waxy solid (with a tint of yellow);

$[\alpha]_D^{25}$ + 0.17 (*c* 15.1, $CHCl_3$); $\mathbf{R}_f$ 0.80 (petroleum ether / EtOAc (10 %)); **IR** (thin film, ν_{max} / cm^{-1}) 3014, 2917, 2849, 1735; **^{1}H NMR** (400 MHz, $CDCl_3$) δ_H 5.46 − 5.22 (11H, m, 10 × =C*H* and C*H*OCO), 4.29 (2H, dd, *J* = 12.0 and 4.0 Hz, 2 × CH_2OCO), 4.18 − 4.11 (2H, m, 2 × CH_2'OCO), 2.90 − 2.75 (8H, m, 4 × =CCH_2C=), 2.37 − 2.26 (6H, m, 3 × CH_2COO), 2.16 − 2.03 (4H, m, =CCH_2CH$_3$ and = CCH_2CH$_2$), 1.70 (2H, quin, *J* = 7.5 Hz, =CCH$_2$CH_2CH$_2$COO), 1.65 − 1.55 (4H, m, 2 × CH_2CH$_2$COO), 1.36 − 1.18 (48H, m, 24 × CH_2), 0.98 (3H, t, *J* = 7.5 Hz, =CCH$_2$CH_3), 0.88 (6H, t, *J* = 7.0 Hz, 2 × CH_3); **^{13}C NMR** (101 MHz, $CDCl_3$) δ_C 173.3, 173.0, 172.9, 132.0, 129.0, 128.8, 128.6, 128.3, 128.2, 128.1, 128.0, 127.9, 127.0, 68.9, 62.2, 62.1, 34.2, 34.1, 33.4, 31.9, 29.7, 29.6, 29.5, 29.4, 29.3, 29.2, 29.1, 29.0, 28.9, 26.5, 25.6, 25.5, 24.9, 24.8, 24.7, 22.7, 20.6, 14.3, 14.1; **HRMS** (ESI+) calc. for $C_{55}H_{96}O_6Na$ [M + Na]$^+$ 875.7099, found 875.7101.

*2.1.2.19. 1-(5Z,8Z,11Z,14Z,17Z)-Eicosa-5,8,11,14,17-pentaenoyl)-2,3-dihexadecanoyl-sn-glycerol, (S)-**5a**.* (*S*)-**5a** was prepared using General Procedure C, and the spectroscopic data was identical to that obtained for (*R*)-**5a**. For further details, please see *Supplementary material*.

*2.1.2.20. 3-(5Z,8Z,11Z,14Z,17Z)-Eicosa-5,8,11,14,17-pentaenoyl)-1,2-dioctadecanoyl-sn-glycerol, (R)-**5b**.* (*R*)-**5b** was prepared using General Procedure C, with (*S*)-**3b** (301 mg, 0.48 mmol), EPA (170 μL, 0.53 mmol, 1.1 equiv.), EDCI (111 mg, 0.58 mmol, 1.2 equiv.) and DMAP (14.0 mg, 0.12 mmol, 0.2 equiv.) in CH_2Cl_2 (1.2 mL). Purification *via* column chromatography (petroleum ether / EtOAc (5 %) gave (*R*)-**5b** (413 mg, 0.45 mmol, 94 %) as a white waxy solid (with a tint of yellow);

$[\alpha]_D^{25}$ + 0.18 (*c* 12.3, $CHCl_3$); $\mathbf{R}_f$ 0.70 (petroleum ether / EtOAc (10 %)); **IR** (thin film, ν_{max} / cm^{-1}) 3013, 2917, 2849, 1735; **^{1}H NMR** (400 MHz, $CDCl_3$) δ_H 5.45 − 5.23 (11H, m, 10 × =C*H* and C*H*OCO), 4.36 − 4.22 (2H, m, 2 × CH_2OCO), 4.18 − 4.11 (2H, m, 2 × CH_2'OCO), 2.90 − 2.75 (8H, m, 4 × =CCH_2C=), 2.40 − 2.25 (6H, m, 3 × CH_2COO), 2.17 − 2.02 (4H, m, =CCH_2CH$_3$ and = CCH_2CH$_2$), 1.70 (2H, quin, *J* = 7.5 Hz, =CCH$_2$CH_2CH$_2$COO), 1.65 − 1.56 (4H, m, 2 × CH_2CH$_2$COO), 1.38 − 1.18 (56H, m, 28 × CH_2), 0.97 (3H, t, *J* = 7.5 Hz, =CCH$_2$CH_3), 0.88 (6H, t, *J* = 7.0 Hz, 2 × CH_3); **^{13}C NMR** (101 MHz, $CDCl_3$) δ_C 173.4, 173.2, 173.0, 132.2, 129.1, 128.9, 128.7, 128.4, 128.3, 128.2, 128.0, 127.2, 69.0, 62.4, 62.3, 34.4, 34.2, 33.6, 32.1, 29.9, 29.8, 29.7, 29.6, 29.5, 29.4, 29.3, 29.2, 29.1, 29.0, 26.7, 25.8, 25.7, 25.1, 25.0, 24.9, 22.9, 20.7, 14.4, 14.3; **HRMS** (ESI+) calc. for $C_{59}H_{104}O_6Na$ [M + Na]$^+$ 931.7725, found 931.7701.

*2.1.2.21. 1-(5Z,8Z,11Z,14Z,17Z)-Eicosa-5,8,11,14,17-pentaenoyl)-1,2-dioctadecanoyl-sn-glycerol, (S)-**5b**.* (*S*)-**5b** was prepared using General Procedure C, and the spectroscopic data was identical to that obtained for (*R*)-**5b**. For further details, please see *Supplementary material*.

*2.1.2.22. 3-(4Z,7Z,10Z,13Z,16Z,19Z)-Docosa-4,7,10,13,16,19-hexaenoyl)-1,2-dihexadecan-oyl-sn-glycerol, (R)-**6a**.* (*R*)-**6a** was prepared using General Procedure C, with (*S*)-**3a** (331 mg, 0.58 mmol), DHA (213 μL, 0.61 mmol, 1.05 equiv.), EDCI (122 mg, 0.64 mmol, 1.1 equiv.) and DMAP (14.0 mg, 0.12 mmol, 0.2 equiv.) in CH_2Cl_2 (1.5 mL). Purification *via* column chromatography (petroleum ether / EtOAc (5 %) gave (*R*)-**6a** (512 mg, 0.58 mmol, 99 %) as a white waxy solid (with a tint of yellow);

$[\alpha]_D^{25}$ + 0.08 (*c* 13.5, $CHCl_3$); $\mathbf{R}_f$ 0.70 (petroleum ether / EtOAc (10 %)); **IR** (thin film, ν_{max} / cm^{-1}) 3014, 2917, 2849, 1734; **^{1}H NMR** (400 MHz, $CDCl_3$) δ_H 5.46 − 5.23 (12H, m, 12 × =C*H* and C*H*OCO), 4.29 (2H, dd, *J* = 12.0 and 4.5 Hz, 2 × CH_2OCO), 4.20 − 4.10 (2H, m, 2 ×

CH_2'OCO), 2.91 − 2.76 (10H, m, 5 × $=CCH_2C=$), 2.43 − 2.35 (4H, m, $=CCH_2CH_2COO$), 2.31 (2H, t, J = 7.5 Hz, CH_2COO), 2.30 (2H, t, J = 7.5 Hz, CH_2COO), 2.08 (2H, quin, J = 7.5 Hz, $=CCH_2CH_3$), 1.67 − 1.55 (4H, m, 2 × CH_2CH_2COO), 1.36 − 1.18 (48H, m, 24 × CH_2), 0.97 (3H, t, J = 7.5 Hz, $=CCH_2CH_3$), 0.88 (6H, t, J = 7.0 Hz, 2 × CH_3); **^{13}C NMR** (101 MHz, $CDCl_3$) δ_C 173.3, 172.9, 172.5, 132.0, 129.5, 128.6, 128.5, 128.4, 128.3, 128.2, 128.1, 128.0 127.9, 127.7, 127.0, 68.6, 62.3, 62.1, 34.2, 34.1, 33.9, 31.9, 29.9, 29.8, 29.7, 29.6, 29.5, 29.4, 29.3, 29.2, 29.1, 29.0, 25.6, 25.5, 25.4, 24.9, 24.8, 22.7, 22.6, 20.6, 14.3, 14.1; **HRMS** (ESI+) calc. for $C_{57}H_{98}O_6Na$ $[M + Na]^+$ 901.7256, found 901.7256.

*2.1.2.23. 1-(4Z,7Z,10Z,13Z,16Z,19Z)-Docosa-4,7,10,13,16,19-hexaenoyl)-2,3-dihexadecan-oyl-sn-glycerol, (S)-**6a**.* (*S*)-**6a** was prepared using General Procedure C, and the spectroscopic data was identical to that obtained for (*R*)-**6a**. For further details, please see *Supplementary material*.

*2.1.2.24. 3-(4Z,7Z,10Z,13Z,16Z,19Z)-Docosa-4,7,10,13,16,19-hexaenoyl)-1,2-dioctadecan-oyl-sn-glycerol, (R)-**6b**.* (*R*)-**6b** was prepared using General Procedure C, with (*S*)-**3b** (100 mg, 0.16 mmol), DHA (67.0 μL, 0.19 mmol, 1.2 equiv.), EDCI (35.0 mg, 0.18 mmol, 1.1 equiv.) and DMAP (5.0 mg, 0.04 mmol, 0.3 equiv.) in CH_2Cl_2 (0.4 mL). Purification *via* column chromatography (petroleum ether / EtOAc (5 %) gave (*R*)-**6b** (139 mg, 0.15 mmol, 94 %) as a white waxy solid (with a tint of yellow);

$[\alpha]_D^{25}$ +0.10 (*c* 10.1, $CHCl_3$); $\mathbf{R}_f$ 0.70 (petroleum ether / EtOAc (10 %)); **IR** (thin film, ν_{max} / cm^{-1}) 3013, 2917, 2849, 1735; **^{1}H NMR** (400 MHz, $CDCl_3$) δ_H 5.45 − 5.23 (13H, m, 12 × $=CH$ and $CHOCO$), 4.30 (2H, dd, J = 12.0 and 4.0 Hz, 2 × CH_2OCO), 4.21 − 4.10 (2H, m, 2 × CH_2'OCO), 2.91 − 2.75 (10H, m, 5 × $=CCH_2C=$), 2.41 − 2.36 (4H, m, $=CCH_2CH_2COO$), 2.31 (2H, t, J = 7.5 Hz, CH_2COO), 2.30 (2H, t, J = 7.5 Hz, CH_2COO), 2.12 − 2.03 (2H, m, $=CCH_2CH_3$), 1.66 − 1.56 (4H, m, 2 × CH_2CH_2COO), 1.38 − 1.18 (56H, m, 28 × CH_2), 0.97 (3H, t, J = 7.5 Hz, $=CCH_2CH_3$), 0.88 (6H, t, J = 7.0 Hz, 2 × CH_3); **^{13}C NMR** (101 MHz, $CDCl_3$) δ_C 173.4, 173.0, 172.7, 132.2, 129.6, 128.6, 128.5, 128.4, 128.3, 128.2, 128.1, 128.0, 127.9, 127.8, 127.0, 69.0, 62.4, 62.2, 34.4, 34.2, 34.1, 32.1(2), 29.9, 29.8(2), 29.7, 29.6, 29.5, 29.4, 29.3, 29.2, 29.1, 29.0, 25.8, 25.7, 25.1, 25.0, 24.9, 22.9, 22.8, 20.7, 14.4, 14.3; **HRMS** (ESI+) calc. for $C_{61}H_{106}O_6Na$ $[M + Na]^+$ 957.7882, found 957.7880.

*2.1.2.25. 1-(4Z,7Z,10Z,13Z,16Z,19Z)-Docosa-4,7,10,13,16,19-hexaenoyl)-2,3-dioctadecan-oyl-sn-glycerol, (S)-**6b**.* (*S*)-**6b** was prepared using General Procedure C, and the spectroscopic data was identical to that obtained for (*R*)-**6b**. For further details, please see *Supplementary material*.

2.2. HPLC enantiomer resolution and enantiopurity analysis

2.2.1. Materials and reagents

The enantiostructured TAGs (*sn*-16:0-16:0-DHA, *sn*-DHA-16:0-16:0, *sn*-18:0-18:0-DHA, *sn*-DHA-18:0-18:0, *sn*-16:0-16:0-EPA, *sn*-EPA-16:0-16:0, *sn*-18:0-18:0-EPA, *sn*-EPA-18:0-18:0, *sn*-16:0-16:0-ALA, *sn*-ALA-16:0-16:0, *sn*-18:0-18:0-ALA and *sn*-ALA-18:0-18:0) were analyzed by using chiral-phase LC method to investigate their chromatographic elution behavior in the chiral environment and to confirm the enantiopurity. All samples were diluted to hexane or to a mixture of hexane and isopropanol (3:2, v/v). Both solvents were HPLC grade and purchased from VWR International (Radnor, PA). One enantiomer of each synthesized enantiopair was analyzed as such to get the retention times and to automate the switching between the columns. Enantiopairs were analyzed as a mixture of 75 %:25 % to determine their enantiomeric separation and the elution order and as an enantiomeric mixture of 99 %:1 % to study the enantiopurity.

2.2.2. HPLC instrumentation

To improve the chromatographic separation by increasing the column length, chiral recycling HPLC (R-HPLC) method described previously (Kalpio et al., 2015) was applied, using two polysaccharide-based chiral stationary phases, CHIRALCEL OD-RH (150 × 4.6 mm, 5 μm, Chiral Technologies Europe, Illkirch, France), in polar-organic phase mode. A precolumn (10 × 4.0 mm, 5 μm) was connected outside to equalize the cycles. Methanol (Sigma-Aldrich Corporation, St. Louis, MO) was used as a mobile phase and isopropanol as the washing solution. The column temperature was 25 °C, flow rate 0.5 mL/min, and injection volume 10 μL. Before injections, samples were diluted to isopropanol to a concentration of 1 mg/mL. The samples were detected using a UV detector at 205 nm. The sample recycling system with a ten-position valve allowed analytes to alternate between two similar chiral columns enabling enantioseparation. Once timed separately for each enantiopair by used input, the switching between two columns was automated. Before enantiomeric resolution, good chromatographic performance, including peak shape and width, was ensured. The flow rate of the mobile phase and sample size were optimized to narrow down the peak width. With the R-HPLC configuration containing two columns, the influence of flow rate on column pressure was followed carefully.

2.2.3. Data treatment

The peak areas were integrated using a LabSolutions 5.57 software (Shimadzu, Kyoto, Japan). The following data analysis parameters were used: width 200 s, slope 150–200 μV/min, drift 0 (automatic) and minimum area 1000 counts. Due to the different enantiomeric resolution, the value for slope had to be adjusted. However, the similar data analysis parameters for each enantiopair were applied, and consequently, the results were comparable. Within each enantiopair, the peak area ratio was regarded as the ratio of concentrations between the two enantiomers separated. For calculations, the average value of 2–4 last peak pairs was used depending on the efficiency of enantiomeric separation (Table 3).

Enantiomeric resolution (R_s) was calculated by the instrument software according to Eq. (1).

$$\textit{Enantiomeric resolution},\ R_S = \frac{2(t_{R2} - t_{R1})}{W + W_p} \quad (1)$$

where t_{R1} = retention time, t_{R2} = retention time of previous peak, W = peak width, W_p = peak width of previous peak

The peak width (W) is the time between two intersection points on the baseline by the tangent lines drawn from the left and right inflection of a peak.

Enantiopurity. There are different calculation procedures for enantiopurity due to the different methods used for determination. IUPAC defines enantiopurity as enantiomer excess (Moss, 2009), and thus the calculations were made according to Eq. (2) (Morante-Zarcero et al., 2009).

$$\textit{Enantiomer excess},\ ee(\%) = \left(\frac{[t_{ri}] - [t_{rii}]}{[t_{ri}] + [t_{rii}]}\right) \times 100 \quad (2)$$

where $[t_{ri}]$ and $[t_{rii}]$ are the relative ratios of areas of the major and minor enantiomers, respectively. The areas were automatically determined by LabSolution software. The ee (%) was calculated by first summing the areas of both peaks and determining their relative ratios.

Impurity assessment. In addition, the proportion of impurity can be calculated (Eq. 3).

$$\textit{Proportion of Impurity}\ (Area\%) = \left(\frac{[t_{rii}]}{[t_{ri}] + [t_{rii}]}\right) \times 100 \quad (3)$$

, where $[t_{ri}]$ and $[t_{rii}]$ are as stated before.

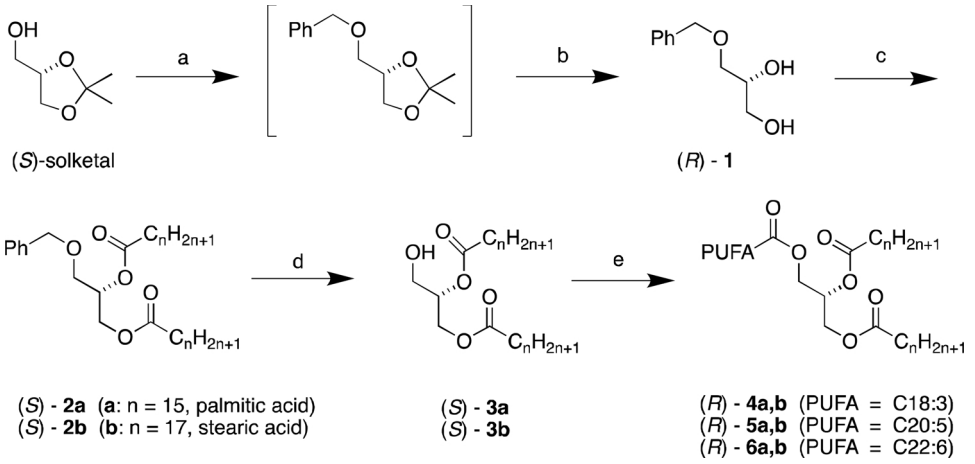

Scheme 1. The synthetic route for the structured TAGs (shown for the *R*-enantiomers) commencing from (*S*)-solketal. *Reagents and conditions*: (a) NaH, THF, then BnBr; (b) 1 M HCl, H_2O/EtOH, reflux30 min.; (c) Palmitic or stearic acid, CAL-B, vacuum, 80 °C; (d) H_2, 10 % Pd/C, cat. $HClO_4$, THF/pet. ether, r.t.; (e) PUFA, EDCI, DMAP, CH_2Cl_2, r.t.

3. Results and discussion

3.1. Synthesis

The synthetic route illustrated in Scheme 1 was followed for the synthesis of the structured TAGs (shown for the *R*-enantiomers) commencing from (*S*)-solketal. This is a very similar approach to the one that was followed in our previously described synthesis of enantiopure AAB type TAGs possessing two identical saturated fatty acyl groups (palmitic or stearic acids) along with one unsaturated fatty acid, either as oleic acid or linoleic acid (Kristinsson et al., 2014). In that case no enzyme was involved and the EDCI coupling agent was used to introduce the saturated fatty acyl groups chemically into the *sn*-3 and *sn*-2 positions of the benzylated glycerol adduct (*S*)-**1**, whereas in the current approach this was executed enzymatically by use of immobilized *Candida antarctica* lipase (CAL). In the final step, the pure n-3 PUFAs (ALA, EPA and DHA) were introduced to the *sn*-1 terminal position by Steglich esterification by use of the EDCI coupling agent after removal of the benzyl protective moiety by catalytic hydrogenolysis over Pd/C.

Referring to Scheme 1 the benzyl-protected glycerol derivatives (*R*)-**1** and the corresponding (*S*)-**1** were accomplished by a previously described two-step procedure (Kristinsson et al., 2014), starting from (*S*)- and (*R*)-solketals, respectively, and obtained in excellent yields (94 and 95 % over the two steps, respectively). Palmitic acid or stearic acid was introduced to both hydroxyl groups of (*R*)-**1** by use of CAL-B to accomplish benzyl protected (*S*)-**2a** (palmitic acid) and (*S*)-**2b** (stearic acid) in excellent yields, 97 and 92 %, respectively. In our previous report these derivatives were prepared by aid of EDCI coupling agent and were not purified prior to the debenzylation. The enzymatic reaction was performed without solvent under vacuum at 80 °C. It took 24 h for the reaction to proceed to completion and in this reaction, we have firm reasons to believe that the fatty acids were incorporated into the 2-position by acyl-migration, promoted by the high temperature and the presence of protons from the fatty acids (Haraldsson et al., 1995). The diacylated adducts (*S*)-**2a** and (*S*)-**2b** were isolated and purified by crystallization from ethanol. Similarly, the corresponding antipodal adducts (*R*)-**2a** and (*R*)-**2b** were obtained in 95 and 80 % yields, respectively.

As before, deprotection of the benzyl moiety was executed by catalytic hydrogenolysis over Pd/C by aid of catalytic amounts of perchloric acid (Hartung and Simonoff, 1953; Rylander, 1990). The deprotection took place very cleanly with no sign of acyl-migration as was firmly established by 400 MHz ^{1}H and ^{13}C NMR spectroscopy analysis. That technique is of great use to monitor a full regiocontrol of reactions involving 1,3- and 1,2-DAGs as well as 1- and 2-MAGs as has been described in details in previous reports (Halldorsson et al., 2003; Magnusson and Haraldsson, 2012, 2010). There were no indications of any 1,3-DAGs present in the products from the hydrogenolysis reaction. The resulting enantiostructured DAGs (*S*)-**3a** and (*S*)-**3b** were accomplished in 98 and 80 % yields, respectively, after recrystallization from hexane. Similarly, the antipodal (*R*)-derivatives were obtained in 97 and 87 % yields, respectively, for (*R*)-**3a** and (*R*)-**3b**.

In the final step the DAGs (*S*)-**3a**,**b** and (*R*)-**3a**,**b** were acylated with ALA, EPA and DHA to achieve the corresponding (*R*)- and (*S*)-**4a**,**b**, (*R*)- and (*S*)-**5a**,**b** and (*R*)- and (*S*)-**6a**,**b**, respectively, using EDCI as a coupling agent in presence of DMAP in dichloromethane at r.t. All products were obtained in excellent yields after purification by silica gel column chromatography, except (*S*)-**5b** that was accomplished in 82 % yield. Table 1 reveals the yields and specific optical rotation values for the enantiostructured TAG products (*R*)-**4a**,**b - 6a**,**b** and the (*S*)- **4a**,**b - 6a**,**b** antipods. All these compounds were fully characterized by 400 MHz ^{1}H and ^{13}C NMR and IR spectroscopy analyses and their high-resolution

Table 1
The identities of the enantiostructured TAG products (*S*)-**4a**,**b – 6a**,**b** and (*R*)-**4a,b – 6a,b**, constituting pure ALA (**4**), EPA (**5**) and DHA (**6**) together with palmitic (**a**) and stearic (**b**) acids, along with their obtained yields and specific optical rotations.

Product	*sn*-1	*sn*-2	*sn*-3	Abbreviation	Yield (%)	$[a]_D^{20}$
(*S*)-**4a**	ALA	$C_{15}H_{31}COO$-	$C_{15}H_{31}COO$-	*sn*-ALA-16:0-16:0	95	−0.02
(*S*)-**4b**	ALA	$C_{17}H_{35}COO$-	$C_{17}H_{35}COO$-	*sn*-ALA-18:0-18:0	96	−0.04
(*R*)-**4a**	$C_{15}H_{31}COO$-	$C_{15}H_{31}COO$-	ALA	*sn*-16:0-16:0-ALA	96	0.02
(*R*)-**4b**	$C_{17}H_{35}COO$-	$C_{17}H_{35}COO$-	ALA	*sn*-18:0-18:0-ALA	96	0.02
(*S*)-**5a**	EPA	$C_{15}H_{31}COO$-	$C_{15}H_{31}COO$-	*sn*-EPA-16:0-16:0	99	−0.17
(*S*)-**5b**	EPA	$C_{17}H_{35}COO$-	$C_{17}H_{35}COO$-	*sn*-EPA-18:0-18:0	82	−0.18
(*R*)-**5a**	$C_{15}H_{31}COO$-	$C_{15}H_{31}COO$-	EPA	*sn*-16:0-16:0-EPA	97	0.17
(*R*)-**5b**	$C_{17}H_{35}COO$-	$C_{17}H_{35}COO$-	EPA	*sn*-18:0-18:0-EPA	94	0.18
(*S*)-**6a**	DHA	$C_{15}H_{31}COO$-	$C_{15}H_{31}COO$-	*sn*-DHA-16:0-16:0	99	−0.17
(*S*)-**6b**	DHA	$C_{17}H_{35}COO$-	$C_{17}H_{35}COO$-	*sn*-DHA-18:0-18:0	99	−0.09
(*R*)-**6a**	$C_{15}H_{31}COO$-	$C_{15}H_{31}COO$-	DHA	*sn*-16:0-16:0-DHA	94	0.08
(*R*)-**6b**	$C_{17}H_{35}COO$-	$C_{17}H_{35}COO$-	DHA	*sn*-18:0-18:0-DHA	93	0.10

mass spectrometry analyses (HRMS) offered satisfactory results. The specific optical rotation values warrant a comment in remaining extremely low. This was to be expected as a result of the cryptoactivity behavior that is characteristic of chiral TAGs that was also observed in our previous studies involving the AAB type TAGs. The cryptoactivity term refers to compounds displaying specific rotation remaining close to zero and hardly measureable (Foss et al., 2005; Schlenk, 1965). Baer and Fischer were the first to report such behavior for TAGs in the late 1930s (Baer and Fischer, 1939; Fischer and Baer, 1941). As can be noticed from the results in Table 1 the specific optical rotation absolute values ranged between 0.02 to 0.18, lowest for the ALA adducts, however, the signs remained consistent in terms of negative values for all the (*S*)- and positive for the (*R*)-TAGs.

By the methodology described we have also succeeded in synthesizing tens of grams of enantiostructured TAGs possessing pure DHA along with stearic acid (25 g of each of the TAG enantiomers (*R*)- and (*S*)-**6b**) and palmitic acid (50 g each of the (*R*)- and (*S*)-**6a** enantiomers). The former TAGs with DHA and stearic acid have already been submitted to animal bioavailability studies on rats along with 25 g of the corresponding symmetrically ABA structured TAG possessing DHA in the 2-position and stearic acid in the remaining 1,3-positions accomplished by previously described procedures (Linderborg et al., 2019). The corresponding TAGs possessing DHA and palmitic acid syntheses have also been completed (50 g of each TAG type) that will be used in further animal studies. For these large-scale syntheses DHA of purity levels ≥ 95 % was used, whereas in the material intended for the chiral separation studies the purity levels of all n-3 PUFAs including DHA were 99 %.

3.2. Chromatographic results

The adjusted retention times ($t_R = t_R - t_M$) after the first column and equivalent carbon numbers of the TAGs [ECN, defined as the number of carbon atoms in the fatty acid residues (ACN) minus twice the number of DBs] are presented at Table 2.

Both the length of the acyl chain and the number of DBs of the fatty acids have a crucial impact on retention of TAGs. In our previous study, the retention of TAGs decreased with increasing unsaturation and with decreasing acyl chain length when polar mobile phase was used. In the current study, TAGs with C16–C20 fatty acids were eluted in the order of ECN, in agreement with our previous findings (Kalpio et al., 2015). Additionally, the current study showed that presence of an n-3 PUFA with 0–5 DBs in the TAG did not change elution order based on the ECN. However, when the number of DBs increased from 5 (EPA) to 6 (DHA), the elution order of TAGs did not follow the ECN values. TAGs containing DHA with six DBs eluted later than TAGs containing EPA with five DBs, even though the ECN were the same. The main reason is likely the spatial configuration of very long carbon chains of the n-3 PUFAs in the TAG molecules (Řezanka et al., 2018). Řezanka and coworkers also noticed certain abnormalities in the retention with even up to 20 min difference in the retention times of TAGs with the same ECN, when TAGs containing at least one very long chain fatty acid were chromatographed on two chiral (3,5-dimethylphenylcarbamate modified β-cyclodextrin) columns using gradient of hexane and hexane/2-propanol. Despite the different chromatographic conditions applied, similar mechanisms probably explain the elution behavior of DHA-TAGs: the interactions of the DHA enantiomers with the mobile phase and the stationary phase. *Cis*-unsaturated fatty acid tails of DHA-TAGs bent to a greater extent than the less unsaturated PUFAs, due to the higher number of *cis*-double bonds present, each causing a permanent kick and bending in the hydrocarbon chain.

Table 2
Chromatographic results.

Enantiomeric TAG pairs	ECN (= ACN − 2 × DB)	Adjusted retention time, t'_R (min), after the first column
sn-EPA-16:0-16:0	42	19.10
sn-16:0-16:0-EPA	42	19.96
sn-ALA-16:0-16:0	44	21.01
sn-16:0-16:0-ALA	44	21.64
sn-DHA-16:0-16:0	42	21.30
sn-16:0-16:0-DHA	42	22.70
sn-EPA-18:0-18:0	46	29.48
sn-18:0-18:0-EPA	46	30.29
sn-ALA-18:0-18:0	48	31.49
sn-18:0-18:0-ALA	48	32.81
sn-DHA-18:0-18:0	46	33.36
sn-18:0-18:0-DHA	46	35.62

Based on the findings of previous research and the current study, ECN values should be used to predict the order of elution in chiral environment only for TAGs containing long chain PUFAs with 1–5 DBs under similar chromatographic conditions. Even though some systematic behavior can be noticed, it is a challenging task to find any common rule about the elution order of chiral TAGs. This is due to the fact that the chiral recognition mechanisms at molecular level are still not fully understood in the chromatography of lipids. In addition to the traditional comprehensive lipid profiling, one trend of lipidomic studies is to aim for a deeper understanding of a specific lipid class (Yang et al., 2016). Thus, all new information on the chiral retention behavior at the molecular level is essential for further development in the field.

3.3. Enantiomer resolution and elution order

The applied R-HPLC method confirmed the presence of two enantiomers in each of the pairs synthesized. The method was demonstrated to enable the resolution of TAG enantiomers with at least up to six DBs. Resolution of the chiral separation of enantiopairs examined after the last column calculated by the instrument software varied between 1.0 and 3.8 (Fig. 1). Only TAGs containing DHA were separated with one column without recycling, but not to the baseline. The peak shape and area remained constant and the peak broadening did not limit the analysis. Consequently, recycling was continued until the desired resolution was achieved. All enantiopairs were clearly separated after four columns. Previously, less peak broadening and better separation was offered with two identical columns compared to single-column (Liu et al., 2014).

The non-destructive UV–vis detection enabled elucidation of the whole separation. As TAG enantiomers have identical physicochemical properties in an isotropic environment (Sánchez et al., 2012), the detector response is the same for both enantiomers. Usual disadvantages in lipid analysis, namely differences in sensitivity between saturated and unsaturated TAGs and insufficient sensitivity for all saturated TAGs (Holčapek et al., 2005), did not hinder the analysis in this study.

Elution order for SSU/USS type enantiopairs with two saturated and one unsaturated fatty acids was in accordance with earlier findings (Kalpio et al., 2015). The enantiomer with an n-3 PUFA in the *sn*-1 position eluted faster than the enantiomer with the unsaturated fatty acid in the *sn*-3 position. Despite the different retention behavior of DHA-TAGs compared to other TAGs, there was no difference in elution order between DHA-TAG enantiomers. The enantiomeric elution order has been opposite when non-polar solvents like hexane-based mobile phases were used (Lísa and Holčapek, 2013; Řezanka et al., 2018).

3.4. Enantiopurity

With all enantiomers examined the ee (%) was more than 96 % (Table 3). No impurities of the opposite enantiomer were detected from *sn*-ALA-16:0-16:0. The small shoulder of the opposite enantiomer i.e. the peak area of impurity was less than 2 % of the peak area of the actual target compound. Performance of the system to detect small enantiomeric impurities was confirmed using a sample of each enantiomer spiked with 1 % of the opposite enantiomer. When comparing

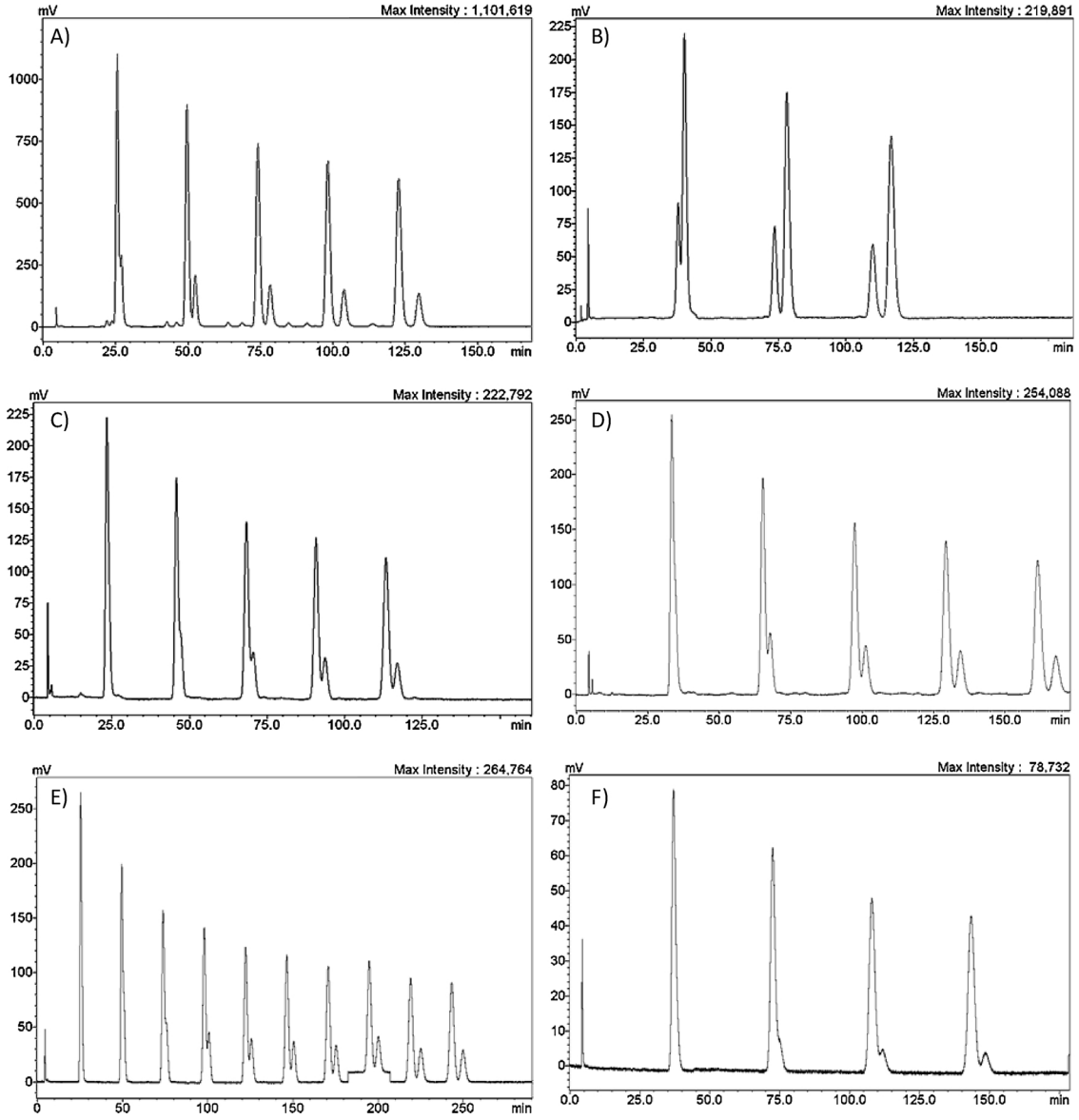

Fig. 1. Chiral R-HPLC-UV chromatogram of six enantiopairs (mixtures of 75 % : 25 %), A) *sn*-DHA-16:0-16:0 co-injected with 25 % of *sn*-16:0-16:0-DHA enantiomer, B) *sn*-18:0-18:0-DHA co-injected with 25 % of *sn*-DHA-18:0-18:0 enantiomer, C) *sn*-EPA-16:0-16:0 co-injected with 25 % of *sn*-16:0-16:0-EPA enantiomer, D) *sn*-EPA-18:0-18:0 co-injected with 25 % of *sn*-18:0-18:0-EPA enantiomer, E) *sn*-ALA-16:0-16:0 co-injected with 25 % of *sn*-16:0-16:0-ALA enantiomer, F) *sn*-ALA-18:0-18:0 co-injected with 25 % of *sn*-18:0-18:0-ALA enantiomer. Columns: CHIRALCEL OD-RH (150 × 4.6 mm, 5 μm), Mobile phase: methanol, Detector: UV SPD-20A at 205 nm.

a chromatogram of enantiostructured TAG with the one spiked with 1 % of the less abundant enantiomer, the opposite enantiomer was clearly visible in the latter (Fig. 2). Fig. 2 illustrates the six column passes of three samples; enantiostructured *sn*-EPA-18:0-18:0, *sn*-EPA-18:0-18:0 spiked with 1 % *sn*-18:0-18:0-EPA and *sn*-EPA-18:0-18:0 spiked with 25 % *sn*-18:0-18:0-EPA. After six columns *sn*-18:0-18:0-EPA is clearly separated from *sn*-EPA-18:0-18:0, and even 1 % impurity is clearly illustrated by comparing the blue chromatogram to black one.

Despite the similar physical and chemical characteristics, enantiomers can and often do exhibit different properties (D'Orazio et al.,

Table 3
Enantiopurity results.

Enantiopairs	ee (%) of the first eluting enantiomer 100 %	ee (%) mixture 99 %:1 %	Proportion of impurity (Area%) / Purity (Area%)
sn-DHA-16:0-16:0 + *sn*-16:0-16:0-DHA	97.7 ± 0.6 (n = 3)	95.1 ± 0.4 (n = 3)	1.2 / 98.8
sn-DHA-18:0-18:0 + *sn*-18:0-18:0-DHA	96.1 ± 0.5 (n = 3)	94.0 ± 0.1 (n = 3)	1.9 / 98.1
sn-EPA-16:0-16:0 + *sn*-16:0-16:0-EPA	98.4 ± 0.3 (n = 2)	97.2 ± 0.5 (n = 2)	0.8 / 99.2
sn-EPA-18:0-18:0 + *sn*-18:0-18:0-EPA	98.2 ± 0.2 (n = 2)	94.5 ± 0.2 (n = 2)	0.9 / 99.1
sn-ALA-16:0-16:0 + *sn*-16:0-16:0-ALA	>99 ± 0 (n = 4)	98.6 ± 0.9 (n = 4)	n.d[a] / 100
sn-ALA-18:0-18:0 + *sn*-18:0-18:0-ALA	98.9 ± 0.2 (n = 3)	97.0 ± 0.5 (n = 4)	tr[b] / 100

[a] n.d; not detected.
[b] tr; trace.

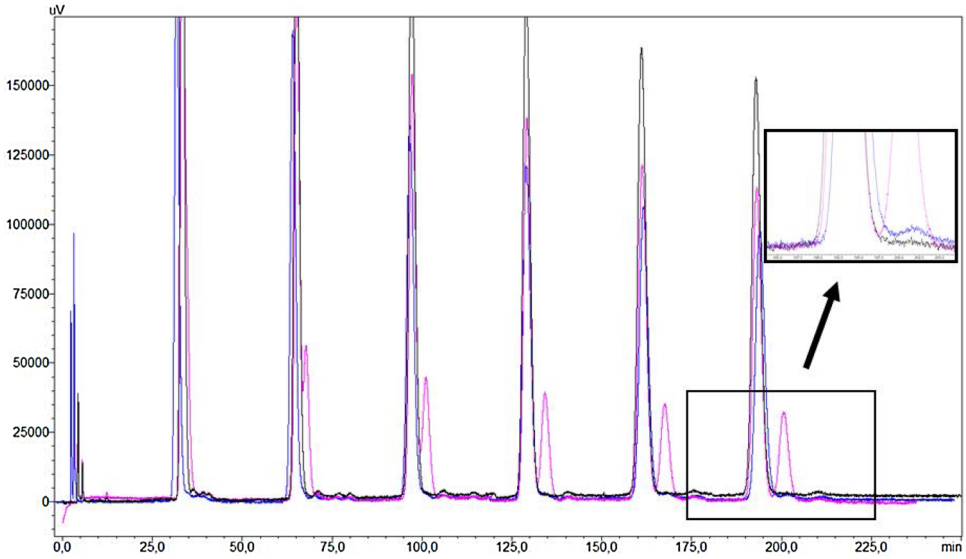

Fig. 2. Chiral R-HPLC-UV chromatogram of *sn*-EPA-18:0-18:0 (black), 99 % *sn*-EPA-18:0-18:0 + 1 % sn-18:0-18:0-EPA (blue), 75 % *sn*-EPA-18:0-18:0 + 25 % *sn*-18:0-18:0-EPA (pink).

2017). Thus, enantiopurity is essential in many applications. In pharmaceutical applications, the methods that determine the specific optical rotation are commonly used for the characterization of the optical purity (Gergely, 2000). The chiroptical techniques like the measurement of optical rotatory dispersion (ORD) and circular dichroism (CD) have also been applied to study saturated glycerides (Gronowitz and Herslof, 1975). Because the optical activity of TAGs is very low, the chiral chromatographic methods have a crucial role in studying enantiopurity. Recently, enantioselective chromatography has been increasingly used not only as a tool for chiral analyses but also as a technique to determine enantiomeric impurities. The R-HPLC can be used to enhance separation efficiency and for example to be applied to study enantiopurity or other impurities in the sample (Liu et al., 2014; Trone et al., 2006). Enantioresolution is the main requirement of the reliable method to study enantiopurity due to the inability of UV detector to detect the co-eluting impurities.

4. Conclusions

Twelve enantiostructured TAGs were successfully synthesized in a five-step chemoenzymatic approach by use of a lipase. Six pairs of TAG enantiomers were formed, all of the AAB type containing one n-3 PUFA (ALA, EPA or DHA) attached to the terminal *sn*-1 or *sn*-3 position of the glycerol backbone along with two palmitic or stearic acids located in the remaining positions. They were all obtained in high chemical purity within very high to excellent yields. These compounds are valuable material for bioavailability studies and as enantiopure reference compounds for chromatographic separation and analysis.

The chiral-phase recycling HPLC (R-HPLC) method enabled resolution of the synthesized TAG enantiomers, and their elution order and chromatographic behavior were firmly established. Elution order of the enantiomers was found to be in agreement with our previous findings determined in our previous study, with the enantiomer with an n-3 PUFA in the *sn*-1 position eluting faster than its enantiomer with the n-3 PUFA in the *sn*-3 position. However, the retention behavior of the TAG enantiomers containing very long chain fatty acid with six DBs (DHA) was different compared to the TAG enantiomers containing C12–C22 fatty acids with 0–5 DBs. Retention of DHA-TAGs was higher than TAGs containing ALA or EPA and they were enantioseparated without recycling. The elution order was based on the ECN for TAGs containing C16–C20 fatty acids with 0–5 DBs. However, DHA-containing TAGs did not follow this elution order. All the DHA-TAGs eluted later than the EPA-TAGs with the same ECN values. Based on the results, we can conclude that no common rules can be applied to predict the elution behavior of all chiral TAGs, which highlights the importance of further studies in the field.

The compounds analyzed with the chiral R-HPLC-UV were all of excellent enantiomeric excess (> 96 %). Among the immense number of molecular species of natural TAGs, only a limited number of TAG reference compounds, and practically no enantiopure TAGs, is commercially available. Thus, reliable and workable synthesis is an obligatory route in order to study the bioactivities of TAG enantiomers and to study the chromatographic behavior of these compounds.

Synthesis of enantiostructured TAGs together with the chiral R-HPLC method enables studies on the role of chirality in food and other biological systems. The knowledge whether a compound is naturally present as a pure enantiomer or with a specific enantiomeric ratio can lead to speculations on the importance of the enantiospecificity for a certain function. The stereospecific information on TAGs offers a new platform for investigations into lipid synthesis and metabolism.

Author contributions

All authors have given approval to the final version of the manuscript.

Declaration of Competing Interest

The authors declare no competing financial interest.

Acknowledgements

The authors thank Jani Sointusalo at University of Turku for assistance with the recycling system, Dr. Sigridur Jonsdottir at the Science Institute, University of Iceland, for the accurate mass measurements, Novozymes AS in Denmark for the lipase and Olav Thorstad of Pronova BioPharma ASA in Norway for pure DHA. The work was funded by the Academy of Finland (Decision Nos. 310982 and 315274), and the Finnish Cultural Foundation. Haraldur G. Gudmundsson acknowledges financial support for a temporary postdoctoral research at University of Turku and Jóhann D. Magnússon financial support from Lýsi hf. in Iceland.

We express our special gratitude to Professor Arnis Kuksis on occasion of his 90th birthday for his guidance and support over the years in the area of lipid research.

Appendix A. Supplementary data

Supplementary material related to this article can be found, in the online version, at doi:https://doi.org/10.1016/j.chemphyslip.2020.104937.

References

Baer, Erich., Fischer, H.O.L., 1939. Studies on acetone-glyceraldehyde. VII. Preparation of l-Glyceraldehyde and l(-)Acetone glycerol. J. Am. Chem. Soc. 61, 761–765. https://doi.org/10.1021/ja01873a001.

Brockerhoff, H., 1971. Stereospecific analysis of triglycerides. Lipids 6, 942–956.

Compton, D.L., Laszlo, J.A., Appell, M., Vermillion, K.E., Evans, K.O., 2012. Influence of fatty acid desaturation on spontaneous acyl migration in 2-Monoacylglycerols. J. Am. Oil Chem. Soc. 89, 2259–2267. https://doi.org/10.1007/s11746-012-2113-z.

D'Orazio, G., Fanali, C., Asensio-Ramos, M., Fanali, S., 2017. Chiral separations in food analysis. TrAC Trends Anal. Chem. 96, 151–171. https://doi.org/10.1016/j.trac.2017.05.013. Special issue on Foodomics and Modern Food Analysis.

Fischer, H.O.L., Baer, Erich., 1941. Preparation and properties of optically active derivatives of glycerol. Chem. Rev. 29, 287–316. https://doi.org/10.1021/cr60093a007.

Foss, B.J., Sliwka, H.-R., Partali, V., Köpsel, C., Mayer, B., Martin, H.-D., Zsila, F., Bikadi, Z., Simonyi, M., 2005. Optically active oligomer units in aggregates of a highly unsaturated, optically inactive carotenoid phospholipid. Chem. - Eur. J. 11, 4103–4108.

Gergely, A., 2000. 6.4. Polarimetry, ORD and CD spectroscopy. In: Görög, S. (Ed.), Progress in Pharmaceutical and Biomedical Analysis, Identification and Determination of Impurities in Drugs. Elsevier, pp. 553–561. https://doi.org/10.1016/S1464-3456(00)80039-3.

Gronowitz, S., Herslof, B., 1975. ORD and CD studies of saturated glycerides. Chem. Phys. Lipids 14, 174–188.

Gudmundsdottir, A.V., Hansen, K.-A., Magnusson, C.D., Haraldsson, G.G., 2015. Synthesis of reversed structured triacylglycerols possessing EPA and DHA at their terminal positions. Tetrahedron 71, 8544–8550. https://doi.org/10.1016/j.tet.2015.09.034.

Halldorsson, A., Magnusson, C.D., Haraldsson, G.G., 2003. Chemoenzymatic synthesis of structured triacylglycerols by highly regioselective acylation. Tetrahedron 59, 9101–9109. https://doi.org/10.1016/j.tet.2003.09.059.

Haraldsson, G.G., Gudmundsson, B.Ö., Almarsson, Ö., 1995. The synthesis of homogeneous triglycerides of eicosapentaenoic acid and docosahexaenoic acid by lipase. Tetrahedron 51, 941–952. https://doi.org/10.1016/0040-4020(94)00983-2.

Haraldsson, G.G., Halldorsson, A., Kulås, E., 2000. Chemoenzymatic synthesis of structured triacylglycerols containing eicosapentaenoic and docosahexaenoic acids. J. Am. Oil Chem. Soc. 77, 1139–1145. https://doi.org/10.1007/s11746-000-0179-1.

Hartung, W.H., Simonoff, R., 1953. Hydrogenolysis of benzyl groups attached to oxygen, nitrogen, or sulfur. Org. React. 7, 263–326.

Holčapek, M., Lísa, M., Jandera, P., Kabátová, N., 2005. Quantitation of triacylglycerols in plant oils using HPLC with APCI-MS, evaporative light-scattering, and UV detection. J. Sep. Sci. 28, 1315–1333.

IUPAC-IUB Commission on Biochemical Nomenclature, 1977. The nomenclature of lipids. Eur. J. Biochem. 79, 11–21. https://doi.org/10.1111/j.1432-1033.1977.tb11778.x.

Kalpio, M., Nylund, M., Linderborg, K.M., Yang, B., Kristinsson, B., Haraldsson, G.G., Kallio, H., 2015. Enantioselective chromatography in analysis of triacylglycerols common in edible fats and oils. Food Chem. 172, 718–724. https://doi.org/10.1016/j.foodchem.2014.09.135.

Kristinsson, B., Linderborg, K.M., Kallio, H., Haraldsson, G.G., 2014. Synthesis of enantiopure structured triacylglycerols. Tetrahedron Asymmetry 25, 125–132.

Laszlo, J.A., Compton, D.L., Vermillion, K.E., 2008. Acyl migration kinetics of vegetable oil 1,2-Diacylglycerols. J. Am. Oil Chem. Soc. 85, 307–312. https://doi.org/10.1007/s11746-008-1202-5.

Linderborg, K.M., Kulkarni, A., Zhao, A., Zhang, J., Kallio, H., Magnusson, J.D., Haraldsson, G.G., Zhang, Y., Yang, B., 2019. Bioavailability of docosahexaenoic acid 22:6(n-3) from enantiopure triacylglycerols and their regioisomeric counterpart in rats. Food Chem. 283, 381–389. https://doi.org/10.1016/j.foodchem.2018.12.130.

Lísa, M., Holčapek, M., 2013. Characterization of triacylglycerol enantiomers using chiral HPLC/APCI-MS and synthesis of enantiomeric triacylglycerols. Anal. Chem. 85, 1852–1859.

Liu, Q., Xiao, J., Yu, J., Xie, Y., Chen, X., Yang, H., 2014. Improved enantioseparation via the twin-column based recycling high performance liquid chromatography. J. Chromatogr. A 1363, 236–241. https://doi.org/10.1016/j.chroma.2014.07.040.

Magnusson, C.D., Haraldsson, G.G., 2010. Chemoenzymatic synthesis of symmetrically structured triacylglycerols possessing short-chain fatty acids. Tetrahedron 66, 2728–2731. https://doi.org/10.1016/j.tet.2010.01.110.

Magnusson, C.D., Haraldsson, G.G., 2012. Activation of n-3 polyunsaturated fatty acids as oxime esters: a novel approach for their exclusive incorporation into the primary alcoholic positions of the glycerol moiety by lipase. Chem. Phys. Lipids 165, 712–720. https://doi.org/10.1016/j.chemphyslip.2012.07.005.

Marchelli, R., Dossena, A., Palla, G., 1996. The potential of enantioselective analysis as a quality control tool. Trends Food Sci. Technol. 7, 113–119. https://doi.org/10.1016/0924-2244(96)10011-X.

Morante-Zarcero, S., del Hierro, I., Fajardo, M., Sierra, I., 2009. HPLC with polysaccharide chiral stationary phase in polar-organic phase mode: application to the asymmetric epoxidation of allylic alcohols. J. Sep. Sci. 32, 3055–3063. https://doi.org/10.1002/jssc.200900170.

Moss, G.P., 2009. Basic terminology of stereochemistry (IUPAC Recommendations 1996). Pure Appl. Chem. 68, 2193–2222. https://doi.org/10.1351/pac199668122193.

Nagai, T., Mizobe, H., Otake, I., Ichioka, K., Kojima, K., Matsumoto, Y., Gotoh, N., Kuroda, I., Wada, S., 2011. Enantiomeric separation of asymmetric triacylglycerol by recycle high-performance liquid chromatography with chiral column. J. Chromatogr. A 1218, 2880–2886. https://doi.org/10.1016/j.chroma.2011.02.067.

Řezanka, T., Kolouchová, I., Nedbalová, L., Sigler, K., 2018. Enantiomeric separation of triacylglycerols containing very long chain fatty acids. J. Chromatogr. A 1557, 9–19. https://doi.org/10.1016/j.chroma.2018.04.064.

Rylander, P.N., 1990. Hydrogenation Methods (Benchtop Edition). Academic Press, London, pp. 158–160.

Sánchez, F.G., Navas Díaz, A., Sánchez Torreño, E., Aguilar, A., Medina Lama, I., Algarra, M., 2012. Determination of enantiomeric excess by chiral liquid chromatography without enantiomerically pure starting standards. Biomed. Chromatogr. BMC 26, 1241–1246. https://doi.org/10.1002/bmc.2685.

Schlenk Jr., Wilhelm W., 1965. Synthesis and analysis of optically active triglycerides. J. Am. Oil Chem. Soc. 42, 945–957.

Smith, S.W., 2009. Chiral toxicology: it's the same thing…Only different. Toxicol. Sci. 110, 4–30. https://doi.org/10.1093/toxsci/kfp097.

Swanson, D., Block, R., Mousa, S.A., 2012. Omega-3 fatty acids EPA and DHA: health benefits throughout life. Adv. Nutr. 3, 1–7. https://doi.org/10.3945/an.111.000893.

Trone, M.D., Vaughn, M.S., Cole, S.R., 2006. Semi-automated peak trapping recycle chromatography instrument for peak purity investigations. J. Chromatogr. A 1133, 104–111.

Vichi, S., Pizzale, L., Conte, L.S., 2007. Stereospecific distribution of fatty acids in triacylglycerols of olive oils. Eur. J. Lipid Sci. Technol. 109, 72–78. https://doi.org/10.1002/ejlt.200600199.

Yang, L., Li, M., Shan, Y., Shen, S., Bai, Y., Liu, H., 2016. Recent advances in lipidomics for disease research. J. Sep. Sci. 39, 38–50. https://doi.org/10.1002/jssc.201500899.

Zawirska-Wojtasiak, R., 2006. Chirality and the nature of food authenticity of aroma. Acta Sci. Pol. Technol. Aliment. 5, 21–36.